DEPARTMENT OF INFORMATICS

TECHNISCHE UNIVERSITÄT MÜNCHEN

Thesis type (Bachelor's Thesis in Informatics, Master's Thesis in Robotics, . . .)

Thesis title

Author

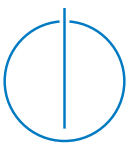

DEPARTMENT OF INFORMATICS

TECHNISCHE UNIVERSITÄT MÜNCHEN

Thesis type (Bachelor's Thesis in Informatics, Master's Thesis in Robotics, . . .)

Thesis title

Titel der Abschlussarbeit

Author:	Author
Supervisor:	Supervisor
Advisor:	Advisor
Submission Date:	Submission date

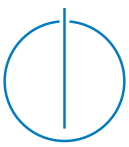

Abstract

Contents

1 Introduction

Machine Learning and Computer Vision has gained much importance in the last years. It can be used in many application fields, such as smart plant monitoring. In this context, it can be used to simplify certain workflows. One example is the hail damage detection of sugar beets.

The idea is to develop a system or application which automatically predicts the damage of plants. This has several advantages, for example less time has to be spent analyzing the fields and possible more accurate results can be achieved.

More concrete, a mobile application was developed, which allows to take images of sugar beet plants. The fotos taken should then be preprocessed and sent to a backend server which analyzes the images and predicts the damage.

In the context of this report, the preprocessing step of such a mobile application is presented. The general idea of the preprocessing step in this application is to standardize the image format of the fotos taken. This means that factors like the number of sugar beet plants, the angle in which the foto was taken and many more things are not often optimal for the model that is predicting the damage. In general, the images that we use for training are taken from directly above the plant in a 90 degrees angle. In the best case, the image only contains one plant which is directly in the center. To be therefore consistent with training images, the new pictures of the plants should ideally be in the same format with similar settings. Therefore, the preprocessing step helps to get better results by standardization of the images.

2 Theoretical Background

There are different types of machine learning algorithms which have various application cases. In this case, an algorithm which performs object detection is used. In the following, the open source architecture YOLO (you only look once) is presented. First, the general principle of object detection is introduced, followed by the description of the architecture of deep YOLO networks. The principle of object detection is to combine Classification with detecting the boundaries of class instances which is exactly what needs to be done in the preprocessing step of sugar beet plants. By detecting the object boundaries of those plants, the image can be cropped to the right size which results in a standardized image format for the following regression task predicting the value of the damage (between 0 and 1).

The state of the art architecture for object detection is YOLO which was first introduced by [1]. Since then, two improved versions were published by the original author. These architectures were called YOLOv2 [2] and YOLOv3 [3]. After that, other authors published the next Version YOLOv4 [4] and also a newest version YOLOv5 can be found.

The advantage of YOLO-networks is that they are much faster than other object detection algorithms like for example R-CNNs [5] which let the model run on a very high number of regions in the image. The idea of YOLO is that the network runs once for the complete image, predicting the bounding boxes and corresponding classes at once. It finds regions in the image which are assigned predicted bounding boxes and probabilities. In the following, the general idea of YOLO is introduced, followed by the incremental improvements in the following versions.

2.1 General Architecture of YOLO

As proposed in the first introduction to YOLO in [1], the network is designed to find objects and the corresponding boxes in a global manner meaning that the image is processed as whole once. Therefore, a $S \times S$ grid divides the image into smaller parts. Each of those cells is responsible to predict B bounding boxes and corresponding confidences. This confidence is defined as $Pr(Object) * IOU_{pred}^{truth}$. The bounding boxes consist of five predictions each, x, y, w, h and the confidence. The first four numbers represent the bounding box with the coordinates of the center (x, y) and the

width and height (both relative to the whole image). Additionally, the cell predicts $Pr(Class_i|Object)$, which are the conditional class probabilities. Only one set of class probabilities are predicted per cell. All in all, the the class probabilities and box confidence predictions are multiplied resulting in the class-specific confidence scores for each box: $Pr(Class_i|Object) * Pr(Object) * IOU_{pred}^{truth} = Pr(Class_i) * IOU_{pred}^{truth}$.

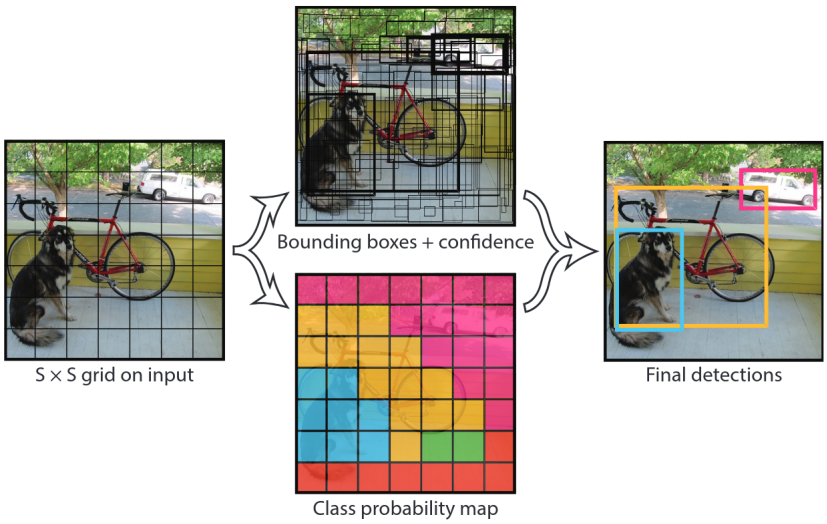

Figure 2.1: Description of idea of YOLO. Taken from [1]

All in all, a tensor of size $S \times S \times (B * 5 + C)$ results. Figure 2.1 depicts the idea of predicting bounding boxes with corresponding classes.

To achieve this, a convolutional neural network is used in combination with fully connected layers. The first part extracts features while the latter part predicts the probabilities and coordinates of the bounding boxes. It consists of 24 convolutional layer and 2 fully connected ones. The concrete network can be seen in figure 2.2.

All in all, the first network has comparable accuracies as other object detection algorithms such as R-CNN or Fast R-CNN. The most important advantage of this architecture is the real time capability. Especially for this preprocessing task, the time plays an important role.

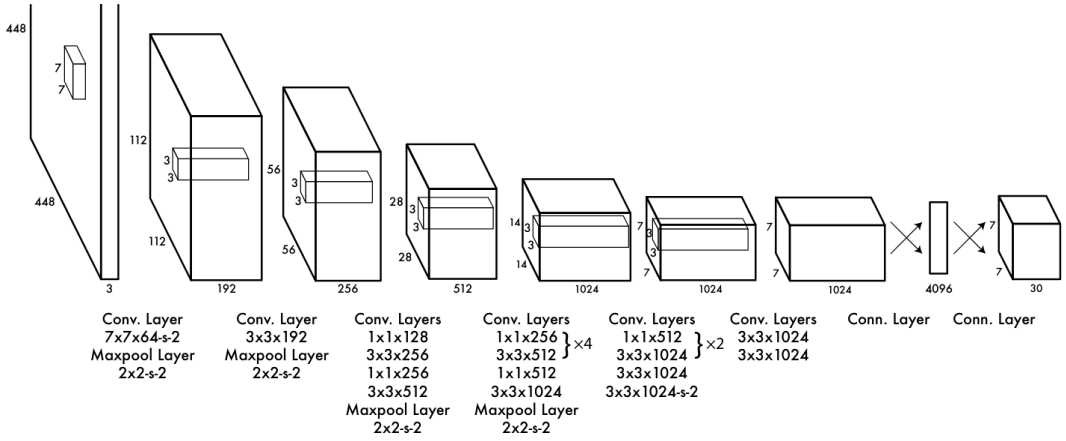

Figure 2.2: Description of network of YOLO. Taken from [1]

2.2 Incremental Improvements

The first architecture was improved incrementally in different versions. The original authors were involved until version 3 ([1]–[3]). After that, other authors published improvements as YOLOv4 [4]. There is no publication to YOLOv5 yet, although there is already an implementation [6].

YOLOv2 With the first improvement which is published in [2], the problem of the localization errors of the boundaries of objects are addressed. The authors call it a better, faster, and stronger version of the YOLO network because of the following improvements.

Depending on the authors, it is made better regarding the recall and localization of bounding boxes. The added batch normalization helps in regularization of the model. The dropout from the model can be left out without overfitting. It is also made better in terms of the image resolution. First, it is trained with the full resolution of 448×448 for 10 epochs. Afterwards, the network is fine tuned on detection. Additionally, the last layers which were originally fully connected ones, are replaced by anchor boxes for the prediction of the bounding boxes. A disadvantage of doing this is that the box dimensions are hand picked. By running k-means clustering on the training set bounding boxes, it can be avoided and good priors can be found automatically. A second disadvantage of using anchor boxes is the instability of the model due to the coordinates of the centers of the boxes. These are calculated depending on the predicted box boundaries. Instead, it is better to predict the location coordinates relative to the

cell's location resulting in values between 0 and 1. Another change is that the feature map is made finer so that the predictions get more accurate. One last change to make the network better is that multi-scale training. Due to the use of convolutional and pooling layers, the input resolution of images can easily be changed. This is used in the training to vary this resolution every few epochs. It makes it all in all more robust and not depending on the input resolution.

Additionally to making the network better, it is also made faster. The authors therefore introduce a new network called darknet-19 as the basis for YOLOv2. It has many advantages compared tp the previous one such as high accuracy and faster times.

To make the network stronger, hierarchical classification is used. Therefore, the principle of subclassing is used. If a concrete dog such as Norfolk terrier is detected, it is also detected as Terrier and dog. Additionally, dataset combination with WordTree is used where multiple datasets are combined. With all this, joint classification and detection is possible meaning that classification and object detection datasets can be used to efficiently train the network.

All in all, this second version of YOLO already brings improvements to the network which is further made better in the next versions.

YOLOv3 The main difference to YOLOv2 is that in the new version presented in [3], a new network architecture for feature extraction is used. It is called Darknet-53 and the structure can be seen in figure 2.3.

It is based on the architecture from YOLOv2 and Darknet-19 and has 53 convolutional layers. It is a deeper network, although the speeds are still much better than other comparable object detection models.

The results show that the accuracy is comparable with ResNet-101 and ResNet-152, Top-5 is even best compared to the others. Additionally, the detectable frames per seconds are much higher than the other models.

YOLOv4 Currently, many object detectors are built up in a similar way. The rough structure can be seen in figure 2.4.

YOLOv4 [4] also consists of such parts. It is a One-Stage Detector and therefore only has dense prediction. As a backbone, CSPDarknet53 [7] is used. The neck consists of SPP (spatial pyramid pooling) [8] and PAN (path aggregation network for instance segmentation) [9]. Finally, the head (dense prediction) is the YOLOv3 network [3]. In addition, it uses some techniques such as data augmentation to improve accuracy for backbone and detector.

All in all, the presented architecture with the additional techniques is superior to other state of the art object detection algorithms in both speed and accuracy.

	Type	Filters	Size	Output
	Convolutional	32	3 × 3	256 × 256
	Convolutional	64	3 × 3 / 2	128 × 128
1×	Convolutional	32	1 × 1	
	Convolutional	64	3 × 3	
	Residual			128 × 128
	Convolutional	128	3 × 3 / 2	64 × 64
2×	Convolutional	64	1 × 1	
	Convolutional	128	3 × 3	
	Residual			64 × 64
	Convolutional	256	3 × 3 / 2	32 × 32
8×	Convolutional	128	1 × 1	
	Convolutional	256	3 × 3	
	Residual			32 × 32
	Convolutional	512	3 × 3 / 2	16 × 16
8×	Convolutional	256	1 × 1	
	Convolutional	512	3 × 3	
	Residual			16 × 16
	Convolutional	1024	3 × 3 / 2	8 × 8
4×	Convolutional	512	1 × 1	
	Convolutional	1024	3 × 3	
	Residual			8 × 8
	Avgpool		Global	
	Connected		1000	
	Softmax			

Figure 2.3: Description of network of YOLOv3. Taken from [3]

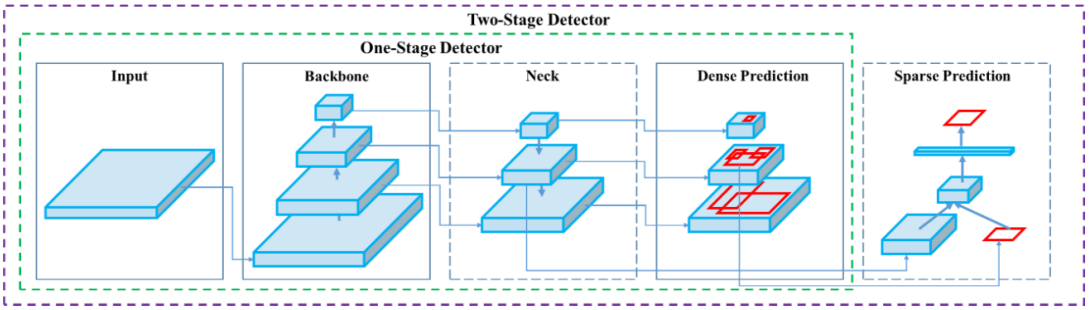

Figure 2.4: Description of network of YOLOv4. Taken from [4]

2.3 Current Architecture YOLOv5

The current version YOLOv5 [6] again has further improvements compared to YOLOv4. The structure is similar to the previous one, also with the same backbone (CSPDarknet 53) and head (YOLOv3). One first difference is that instead of SPP, a faster version SPPF is used which is more than twice as fast. Together with PAN, this builds up the neck part.

Different Network Sizes There are five different network sizes available. They differ in the number of layers and parameters and are called YOLOv5n (nano, smallest), YOLOv5s (small), YOLOv5m (medium), YOLOv5l (large) and YOLOv5x (extra large). Additionally, each of the models

Additional Features As data augmentation, different techniques are used. For example mosaic concatenates several images to one big image. The copy paste technique copies objects from images to other pictures. Additionally, random affine transformations are applied to the images, such as rotations, scaling, translation and shear. Similar to mosaic, MixUp combines different images but with the difference that the pictures are directly laid behind each other. Additional settings like hue, saturation and value are randomly adjusted. Together with random horizontal flips, the variety of the training set is increased which leads to better object detection accuracy.

3 Methodology

To achieve the goal of detecting sugar beet plants, the presented YOLOv5 is used. The exact goal is to develop a preprocessing algorithm which standardizes images of sugar beets for a damage prediction regression task. As described, the images should be standardized in a way that each picture contains one sugar beet plant photographed in a 90 angle to the ground from above. To train the network on the dataset, a nvidia gpu with 24267 MiB memory was used.

In the following, the given dataset, the training of the network, the evaluation of the models and mobile detection will be presented.

3.1 Dataset

There are essentially two sources for images of sugar beets and other plants available. One part consists of images taken in sugar beet fields and the other one is Imagenet [10] where a large number of different images with classes is available.

The number of images of sugar beet plants is 10087. This set can be categorized in two different types. The first type is an image with many small sugar beets. The other one is an image with older and bigger plants where the concrete object boundaries are hard to see. One example for each class can be seen in figure 3.1.

Figure 3.1: Image types

The left one is taken from further away and contains multiple smaller plants. The object boundaries can be seen very clearly. This is not the case for the right example. It contains bigger plants and the boundaries can not be seen clearly because of the neighboring plants. It is not even easy for the human eye to make find the leafs of a distinct plant. The majority of the whole dataset is of the second type (right example). The numbers of images for each type are 9964 for the type of the right example and 123 for the left one. In practice, most images will be of bigger plants because the damage prediction is more important in those cases.

To train the network, the pictures have to be labeled. For each image file, one text-file has to be made which contains the information of the image. For each object, one line with five numbers has to be added. The first one is the class. The second and third one are the coordinates of the center of the bounding box (x- and y-coordinate). These have to be relative to the width and height of the image. The third and fourth ones are the length in x- and y-direction. They also have to be relative to the image's height width. First experiments showed that the labeling has to be done manually to obtain reasonable results. It could be seen that only labeling the images with multiple small plants and annotating the other ones automatically with `0 0.5 0.5 1 1` is not sufficient to detect the exact boundaries of bigger plants. Such a labeling exactly means that the center of the bounding box is in the middle and the boundaries are exactly the same as the image boundaries. In most cases, the whole image was detected as a whole sugar beet plant, which was definitely not the goal. The manual labeling was done with the tool labelImg [11] which provides a graphical user interface to draw the rectangles around the objects. An example of such a labeling of a bigger plant can be seen in figure 3.2.

Figure 3.2: Labeling with labelImg

As you can see in this figure, the plant in the center of the image is labeled as sugar beet. The rectangle of the object has to be as exact as possible to obtain best results in predictions. Although especially in the case of big plants, this is not always easy because neighboring sugar beets are overlapping and the plant boundaries can not even be seen very clearly with the human eye. Nevertheless, all available images were labeled manually to get best possible results. An overview of the complete data set can be seen in table 3.1.

Source	Number images	Image types
TUM	9461	One larger plant
TUM	123	Multiple small plants
Partner	259	Mixed
Drone screenshots	244	Multiple larger plants
Imagenet	2992	Other plants and persons

Table 3.1: Overview over the data set with the available images. Most of them are from TUM and contain about one larger plant.

All in all, the most available images contain about one larger plant from above. The biggest variety of image types can be seen from the Partner. These were taken in very different angles and contain various damages ranging from nearly no to high destruction. The drone screenshots are similar to the TUM data set but are taken from a bit more far above. The drones captured most of the time more than one large plant at a time resulting in overlapping sugar beets again. This overview in the table 3.1 shows that much data was gathered and labeled. Compared to the use case where the plants should be detected, the available data is very suitable for the application as it has many different cases ranging from many plants on one images to only containing one sugar beet. Also the damage classes are distributed.

Additionally, Imagenet was used. 2992 images with other plants, flowers and persons were used. These images were not labeled at all. An exact labeling by hands could have been possible but due to time constraints and the fact that only the boundaries of sugar beets have to be detected exactly, this was not done. Possible other solutions would have been to include multiple other classes like concrete plant types or "person" but this is not needed in this application.

3.2 Training

For the training of the YOLOv5 model, different parameters and other settings have to be specified. One first thing is the decision between different model sizes. As

described in the description of YOLOv5, there are different possibilities. The ones we are concentrating on are the small, medium, and large one. For each of them, a pretrained model on the COCO data set [12] with 300 epochs and default settings are available [6]. This data set contains 328 thousand images with 2.5 million instances of 91 object classes. Alternatively, the raw model without pretraining can be used. In a configuration file, many different hyperparameters can be adjusted such as box, class and obj loss gain. Also the IoU (intersection over union) training threshold can be set. This value determines the fraction of the area of the intersection of two bounding boxes over the union of them. The highest achievable value is 1 which means that the predicted box is exactly the same as the labeled box. Many other parameters for image augmentation are also available. One example therefore is hue, saturation, and value which are then just changed in the image. Also degrees of rotation, translation, scaling, shearing and the perspective can be adjusted. More complex ones are the probability of flipping the image upside down or left-right, respectively. Additionally, mosaic can be chosen. This means that many different images with their labels are concatenated to form a larger image. Also the probability for mixup and copy paste can be chosen independently. Examples for the last three augmentations can be seen in figure 3.3.

Depicted in the top row, mosaic just puts different labeled images together in a random way to form one larger training image. In the middle row, mixup augmentation is depicted. This one is more complex because it copies multiple labeled image overlapping into a larger one. The bottom row depicts the copy paste augmentation which copies single instances of classes to other labeled training images. All in all, these different augmentation strategies help to improve the model's robustness because the variety of input images is increased.

Further settings that have to be made to train the models are defining the train, validation, and testing split. Additionally, the number of epochs can be defined. As optimizer, SGD (stochastic gradient descent), Adam, and AdamW can be chosen. The concrete training scenarios and their settings will be described in the results.

3.3 Inference and Evaluation

For the detection of objects, multiple different inputs are possible. Either the images of whole folders, single pictures, or the live stream of the webcam can be processed. In each way, the image is directly labeled with the bounding box of the detected class. Additionally, it is possible to write the result to a text file in the same format as the label for the training images.

To evaluate the model's accuracies, the test set is used. Metrics like the precision and the recall can be directly measured with the framework [6]. Precision is calculated with $P = \frac{T_p}{T_p+F_p}$ and Recall with $R = \frac{T_p}{T_p+F_n}$ with T_p true positive, F_p false positive, and F_n false negative predictions.

For the three model sizes, different inference times can be observed. For the small one, the predicted takes about 100ms, the medium one takes about 224ms and the slowest is the large one with about 450ms. All times are taken on a normal CPU.

For a live application detecting the objects , the large model is definitely too slow. It takes too much time to detect objects and the live stream updates not fast enough. Even with the medium model, the window is not fluent. Using the small model, a live application detecting the sugar beets can be done. The inference times are not too high to still give a fluent live image.

These inference times leave room for two versions. The first one is just processing the image taken from the field on the server where also the regression model is implemented. The second one is using the model directly in the app so that the user can also see and maybe interact with the bounding boxes of the predicted sugar beets.

3.4 Mobile Detection

For the detection directly in the app, Pytorch mobile [13] can be used. For an overview of machine learning in mobile applications, refer to [14].

For the application, the pt file of the model can be used to detect objects directly in the application. This would have the advantage that the user can directly see whether a sugar beet is detected and adjust his angle or distance to the plant. Additionally possible would be to let the user adjust the bounding box if he thinks that the prediction is not precise enough.

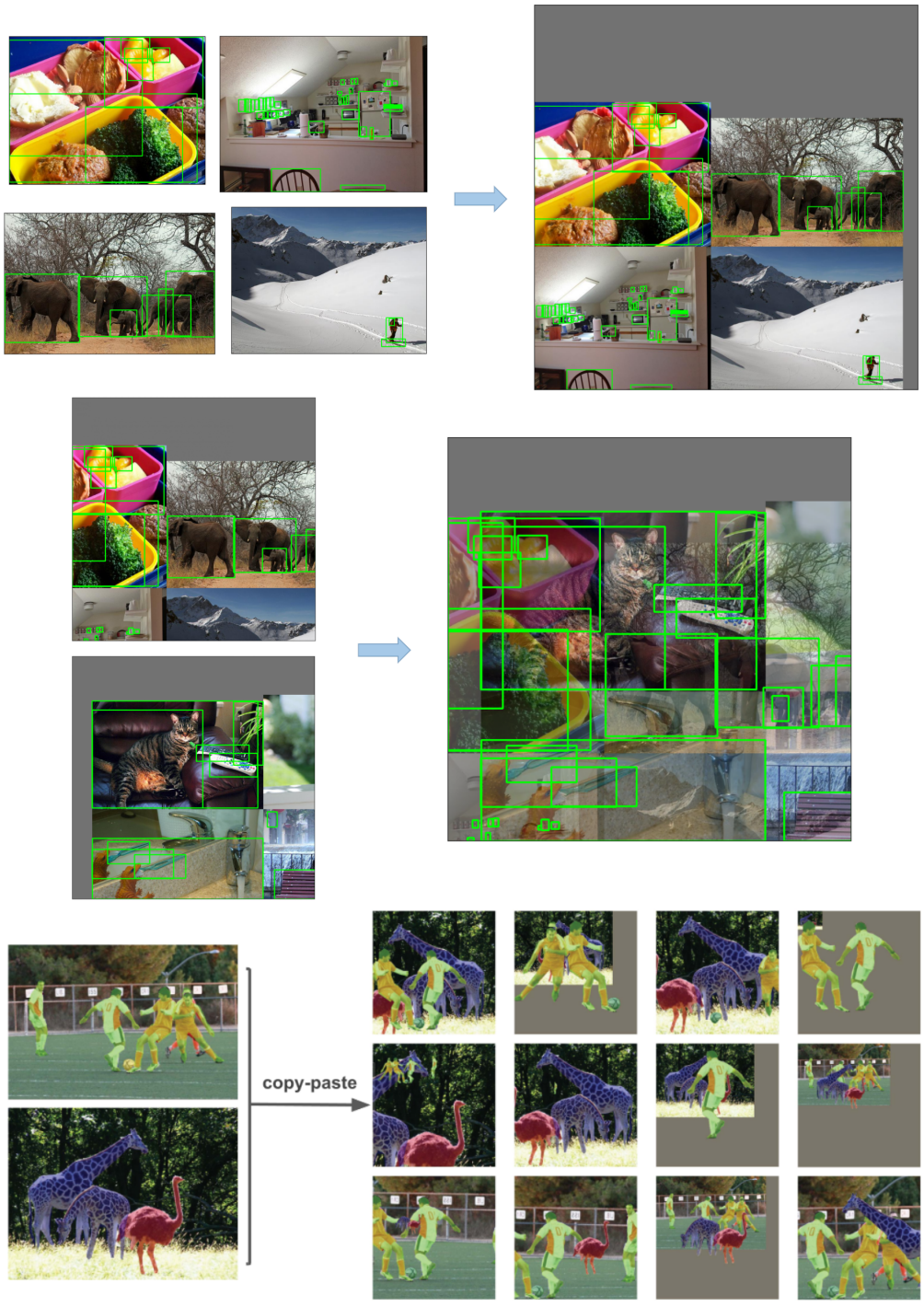

Figure 3.3: Augmentation types, taken from [6]

4 Results

In this chapter, different approaches for training the YOLO model are presented. First, the results of training a simple large model will show a baseline model which is then improved by different settings. Afterwards, the results of training the small and medium model are shown. Finally, the three different model sizes are compared.

4.1 Large Network

The first experiments were made with only a small part of the data set being manually labeled. At first, the images of the TUM data that contain approximately one big sugar beet per image were labeled automatically with `0 0.5 0.5 1 1`. This means that the whole picture is labeled as containing exactly one sugar beet. We assumed that these images were already in the perfect format for our use case and the automatic labeling would be sufficient. The images containing multiple small plants are labeled manually and exactly. The model was trained with default hyperparameters and settings. This means that the number of epochs is 300, box loss gain of 0.05, class loss gain of 0.5, object loss gain of 1.0 and IoU threshold for training of 0.2. The data augmentation values can be found in table 4.1.

Hue	Sat	Value	Degrees	Translate	Scale	Shear	Persp	UD	LR	Mosaic
0.015	0.7	0.4	0.0	0.1	0.5	0.0	0.0	0.0	0.5	1.0

Table 4.1: Values for data augmentation

All in all, small data augmentation is used. 85% of the data was used as training set and 15% as validation set.

For the training and validation set, the results were accurate. With a real number of 9110 sugar beets and a detected number of plants of 8162, this results in an accuracy of $89,6\%$. Although for new, unseen images, the accuracy is very low. Here, the number of labeled sugar beets is 575 and only 68 are detected. An overall accuracy of $11,8\%$ results. In this experiment, only the number of detected and real sugar beets are observed, not the location or size of the bounding boxes. However, the results show that this model

is not sufficient for detecting the boundaries of sugar beets. Two examples of detected objects can be seen in figure 4.1.

Figure 4.1: Examples of detected images.

You can see that in both cases, the whole image is detected as one plant. In the left example, the angle of the recording camera is very good with 90, in the right example which is taken from the Imagenet folder containing sugar beet images, the angle is not perfect. However, also here the whole images is labeled as sugar beet. the class probabilities are 0.95 in the left case and 0.89 in the right image.

Another problem of this model is the high false positive rate in case of other plants. In another test, 1271 images of all kinds of plants of Imagenet are tested. 922 labels of sugar beets were detected which means that about 70% are detected false positive. Two examples can be seen in figure 4.2.

Figure 4.2: Examples of other plants also detected as sugar beets.

You can see that also random plants are detected as sugar beets which should not be the case.

Testing the model with a test set consisting of the heterogeneous Partner data and 400 TUM images which contain multiple small plants and also larger ones, yields the following result which can be seen in figure 4.3.

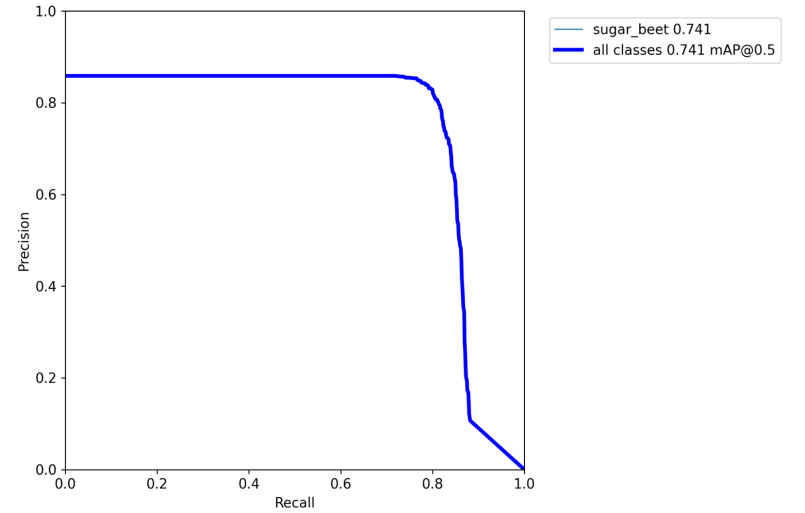

Figure 4.3: P R curve first exp

A perfect model would have an area under curve of 1.0. This one has 0.741 which still has room for improvement.

All in all, we encounter two main problems. The first one is that the bounding boxes of detected plants are just very inaccurate. Most of the time, the whole image is labeled as one sugar beet. The second problem is that the model is not robust. It also detects other plants as sugar beets and it can not distinguish between different kinds of plants.

The first problem can be solved by labeling the data more accurate. By this, the model learns the exact boundaries of sugar beet plants and the predicted results get better. For the second problem, two different solutions exist. One is to add another class called other plant which is essentially everything else than sugar beets. The problem of this is that for example cars or persons are also detected as other plant which is also not intended. The second possible solution of this problem is to add so called background images. These are pictures which are not labeled with any object. Possible images therefore are other plants, persons or cars.

4.2 Small and Medium Network

- small and medium model (from scratch)
- pretrained small model low data augmentation
- improved small model high augmentation

4.3 Comparison

5 Conclusion and Outlook

YOLOv6/YOLOv7, further improvements
Pose detection -> not only bounding box but also pose of person for example

Bibliography

[1] J. Redmon, S. K. Divvala, R. B. Girshick, and A. Farhadi, "You only look once: Unified, real-time object detection," *CoRR*, vol. abs/1506.02640, 2015. arXiv: 1506.02640.

[2] J. Redmon and A. Farhadi, "YOLO9000: better, faster, stronger," *CoRR*, vol. abs/1612.08242, 2016. arXiv: 1612.08242.

[3] ——, "Yolov3: An incremental improvement," *CoRR*, vol. abs/1804.02767, 2018. arXiv: 1804.02767.

[4] A. Bochkovskiy, C.-Y. Wang, and H.-Y. M. Liao, "Yolov4: Optimal speed and accuracy of object detection," *CoRR*, vol. abs/2004.10934, 2020. arXiv: 2004.10934.

[5] R. B. Girshick, J. Donahue, T. Darrell, and J. Malik, "Rich feature hierarchies for accurate object detection and semantic segmentation," *CoRR*, vol. abs/1311.2524, 2013. arXiv: 1311.2524.

[6] *Yolov5 github repository*, https://github.com/ultralytics/yolov5, Accessed: 2022-06-22. DOI: https://doi.org/10.5281/zenodo.3908559.

[7] C.-Y. Wang, H.-Y. M. Liao, Y.-H. Wu, P.-Y. Chen, J.-W. Hsieh, and I.-H. Yeh, "Cspnet: A new backbone that can enhance learning capability of cnn," in *Proceedings of the IEEE/CVF Conference on Computer Vision and Pattern Recognition (CVPR) Workshops*, Jun. 2020.

[8] K. He, X. Zhang, S. Ren, and J. Sun, "Spatial pyramid pooling in deep convolutional networks for visual recognition," *IEEE Transactions on Pattern Analysis and Machine Intelligence*, vol. 37, no. 9, pp. 1904–1916, 2015. DOI: 10.1109/TPAMI.2015.2389824.

[9] S. Liu, L. Qi, H. Qin, J. Shi, and J. Jia, "Path aggregation network for instance segmentation," in *Proceedings of the IEEE Conference on Computer Vision and Pattern Recognition (CVPR)*, Jun. 2018.

[10] J. Deng, W. Dong, R. Socher, L.-J. Li, K. Li, and L. Fei-Fei, "Imagenet: A large-scale hierarchical image database," in *2009 IEEE conference on computer vision and pattern recognition*, Ieee, 2009, pp. 248–255.

[11] *Labelimg*, https://github.com/tzutalin/labelImg, Git code (2015).

[12] T.-Y. Lin, M. Maire, S. J. Belongie, L. D. Bourdev, R. B. Girshick, J. Hays, P. Perona, D. Ramanan, P. Dollár, and C. L. Zitnick, "Microsoft COCO: common objects in context," *CoRR*, vol. abs/1405.0312, 2014. arXiv: 1405.0312.

[13] *Pytorch mobile*, https://pytorch.org/mobile/home/, Accessed: 2022-07-28.

[14] X. Dai, I. Spasić, S. Chapman, and B. Meyer, "The state of the art in implementing machine learning for mobile apps: A survey," in *2020 SoutheastCon*, 2020, pp. 1–8. DOI: 10.1109/SoutheastCon44009.2020.9249652.